Letters in High Energy Physics
ISSN: 2632-2714
Volume 2024

Investigating the Impact of Gas type and Gas Flow Rate on Plasma Jet Parameters by Optical Emission Spectroscopy

Mohammed H. Ahmed[1], Hammad R. Humud[2]

[1, 2]Department of Physics, College of Science, University of Baghdad, Baghdad, IRAQ

[1]Corresponding author: Mohammed.Hawas1604a@sc.uobaghdad.edu.iq
[2]Corresponding author: hamid.r@sc.uobaghdad.edu.iq

Abstract

This study describes the creation of jet plasma at atmospheric pressure with a straightforward plasma jet generation system utilizing air, argon, and nitrogen gases. It comprises a 10 kV high-voltage DC apparatus with a 30 W power output. This research primarily aims to examine the effects of varying the gas flow rate and the gas type (argon, nitrogen, or air) on the microscopic non-thermal plasma features by optical emission spectroscopy (OES). The Boltzmann diagram method was employed to calculate the electron temperature (Te), electron density (ne), and further related quantities, along with other plasma properties. At low flow rates, the electron temperature in argon remains almost constant as the electron density increases, irrespective of the gas flow rate. The electron temperature and nitrogen density exhibit more variation with flow rate. The electron temperature in air exhibits considerable fluctuations with varying flow speeds, although the electron density shows very less variation.

Keywords: Plasma Jet, Plasma Parameters, Non- Thermal Plasma, Optical emission spectroscopy, electron density, electron temperature.

Introduction

The many practical applications of plasma require a system that operates on different gases to be suitable for various industrial, medical, and environmental plasma applications. Non-thermal plasma systems have garnered significant attention in the field of study [1-3]. Plasma is the fourth fundamental state of matter, after solids, liquids, and gases. Plasma can be divided into two categories: thermal and non-thermal plasma. Plasma consists of numerous free electrons and positive and negative ions [4]. One kind of non-thermal atmospheric glow discharge plasma needle, which is operated using a single electrode, used air, nitrogen, and argon gases. The fact that this kind of plasma functions at temperatures close to room temperature means that when plasma comes into contact with an object, it doesn't heat them up. This attribute created the opportunity to use plasma to treat heat sensitive material. The simplicity of use and low cost of atmospheric pressure discharge plasma make them very interesting [5]. Non-thermodynamic (cool plasma) denotes that the temperature of the plasma is not in thermodynamic equilibrium. The temperature of molecules, atoms, and ions does not match the temperature of electrons [6,7]. Because of these properties, Plasma jet systems are versatile tools that can be utilized for a wide range of research purposes it is employed for activating the surface of polymers, developing solar cells, and etching materials [8, 9]. Several uses exist, including the treatment of living cells [10,11]. use cold atmospheric plasma jet treatment of cancer cells [12]. Sterilization [9], blood coagulation [13,14], wound healing [15-19], bacteria activation [20-22], tooth bleaching [23,24], and air purification [25,26] are some of the applications [27]. Air plasma can generate reactive oxygen nitrogen species (RONS). Nitrogen Plasma Technology is a safe and effective technique to achieve significant skin rejuvenation without the dangers and downtime associated with more invasive cosmetic procedures.

Nitrogen gas and ambient air are commonly utilized as working gases in plasma jet systems. Nitrogen is often preferred for its chemical stability and significant reactivity with certain chemicals, despite the widespread availability and cost-

effectiveness of air. Airborne molecules generate reactive species such as ozone, nitric oxide, and nitrogen oxides. In nitrogen, plasma mostly interacts with nitrogen molecules, leading to the generation of nitrogen radicals and ions. Several essential components are required to generate an atmospheric plasma jet. A high-voltage power supply produces plasma discharge; an electrode arrangement begins and maintains the plasma, while a gas distribution system provides gas to the plasma [28,29]. Electrode configurations can be changed to get different plasma forms and properties. For example, a needle-to-plate electrode wire-to-cylinder arrangement can generate a highly focused plasma jet, whereas a wire-to-cylinder layout produces diffuse plasma. Once the atmospheric plasma jet has been produced, its properties can be studied using several diagnostic methods.

The purpose of this study was to examine the characteristics of jet plasma for various gases such as air, nitrogen, and argon. The study focused on determining the electron density (ne) and temperature (Te) for each gas using the optical emission spectroscopy (OES) method. Using the OES methodology allows for precise evaluation of plasma properties and the generation of highly accurate predictions regarding plasma radiation emission [30–34].

The Boltzmann plot method [35-36] was utilized to calculate the electron temperature of plasma:

$$\ln\left[\frac{\lambda_{j_i} I_{ji}}{hc\, A_{j_i g_j}}\right] = -\frac{1}{KT}(E_j) + \ln\left|\frac{N}{U(T)}\right| \ldots\ldots\ldots (1)$$

$\mathbf{I_{ji}}$, and $\mathbf{g_j}$ Represent the relative emission line density between energy levels i and j.
$\mathbf{E_j}$ Is the excitation energy (in eV) for level i.
$\mathbf{A_{ji}}$ Is the possibility of automated radiation transmission from level i to the lower-level j.
$\boldsymbol{\lambda_{ji}}$ Is the wavelength (in nm).
K is the Boltzmann constant.
N is a reference to the population densities of the state.
The following formula can be used to compute Debye's length ($\boldsymbol{\lambda_D}$) [37-38]:

$$\lambda_D = \sqrt[2]{\frac{\varepsilon_O K_B T_E}{n_e e^2}} \quad \ldots\ldots.(2)$$

The plasma frequency is as follows:

$$w_{\rho e} = \sqrt{\frac{e^2 n_e}{\varepsilon_\circ m_e}} \ldots\ldots\ldots (3)$$

Where $\mathbf{m_e}$ It is the electron mass; the following gives the Debye Number ($\mathbf{N_D}$) [39-40]:

$$N_D = \frac{4}{3}\pi\lambda_D^3 n_e \ldots\ldots. (4)$$

2-Experimental part

A simple system for generating plasma jets has been created with air, argon and nitrogen gases. Figure 1 shows the experiment setup which consists of DC high voltage device10 kV, 30watt power output. The electrode at which the plasma is generated consists of a hollow steel tube with an internal diameter of 1.4mm and length of 5cm. At one end of the steel tube, the working gas is connected through a Teflon tube connected to a gas flow rate regulator. The steel tube is wound directly with a high voltage DC power supply. The system was grounded, and the second electrode of the system was connected to the ground.

Plasma is created by applying electrical energy to gas. By doing so, the gas molecules are ionized, causing electrons to separate from the gas molecules. This process generates plasma that has excellent electrical conductivity and can interact with any surface. Plasma can now be used to initiate surface treatment by simply placing any surface in contact with it. To optimize the results of this treatment, we can adjust the effects by choosing the appropriate gas composition and procedure parameters for each specific procedure project.

The plasma jet emissions were evaluated by Suwrit S3000 spectrometer apparatus. The operational range of this device's high resolution spans from 200 nm to 1100 nm. The spectrum from the plasma light was collected and transmitted to the spectrometer via a fiber optic (f600-y-uv-sr-nir) connection. The spectral graph was analyzed utilizing the spectra (version 3.3) software. The x-axis represents the wavelength, while the results indicate the relative strength of the emission peaks recorded by the spectrometer, facilitating the identification of the reactive species in the plasma. Figure 3 illustrates that the spectrometer's fiber

optic was situated near the plasma plume at a constant distance, d. Figure 3 depicts the methodology employed for measuring the working gas during different procedures. The distance between the plasma and the fiber optics was 5 mm. The reactive species in the plasma were represented by the peaks of the spectral bands. Based on the wavelengths, the species in the plasma were determined. When identifying atomic species based on the wavelengths of their wavelengths, the National Institute of Standards and Technology (NIST) (http://www.nist.gov/pml/data/asd.cfm) can be used as a reference source .

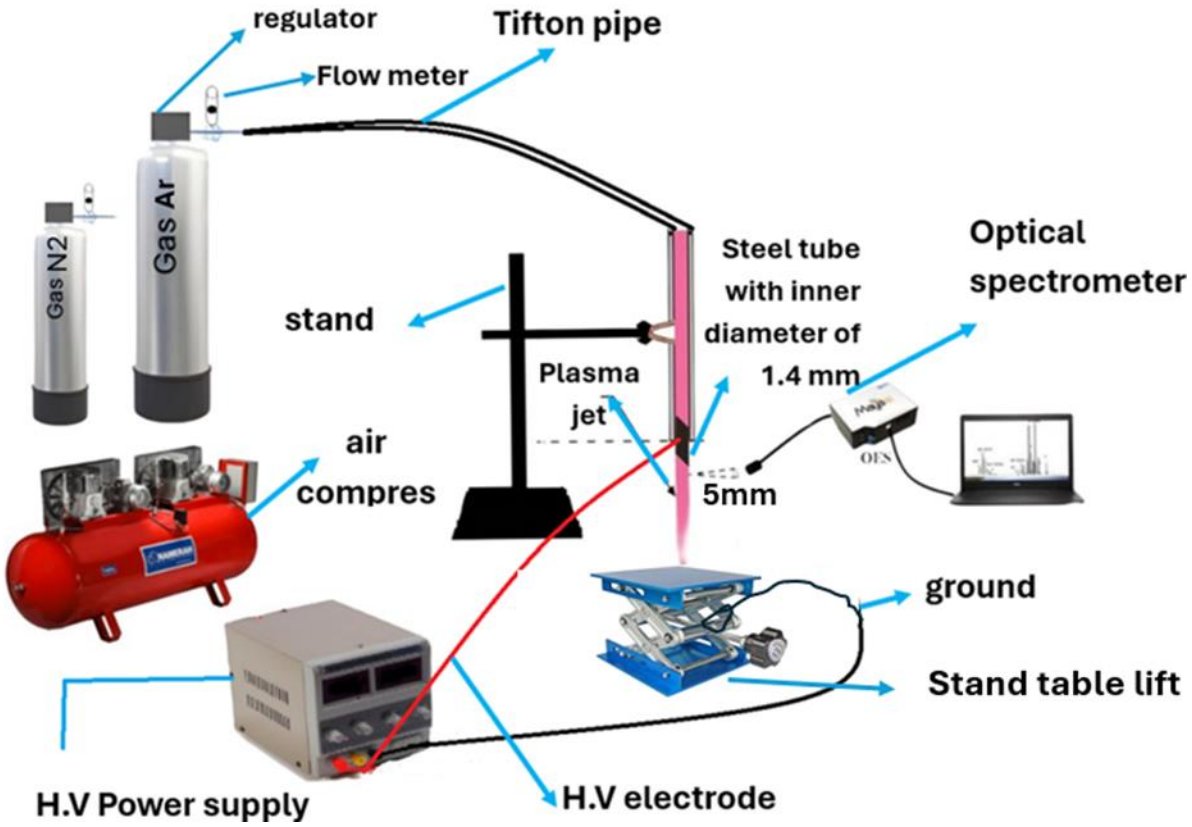

Figure 1: Plasma jet system.

3- The Results

Using spectroscopy is a highly effective diagnostic method for determining the properties of jet plasmas. This study observed the spectral lines emitted by atoms to analyze the impact of various physical parameters on jet plasma formed at atmospheric pressure.Figures 2, 3, and 4 show the relationship between optical emission spectra and gas flow rate for a plasma jet with different gases, Ar, N2, and air.

Figure 2 displays multiple peaks of argon gas in the spectrum, which closely align with the data from the Higher Institute (NIST). At a wavelength of 912.29670 nm, the argon gas (Ar I) consistently exhibits its highest peak in the spectrum, regardless of the gas flow. On the other hand, when the voltage is set at 10 KV and the flow ranges from 1 to 5 L/min, the nitrogen gas (N2 I) reaches its highest peak at a wavelength of 762.81800 nm. The majority of plasma peaks were observed within the wavelength range of 300 to 1000 nm.

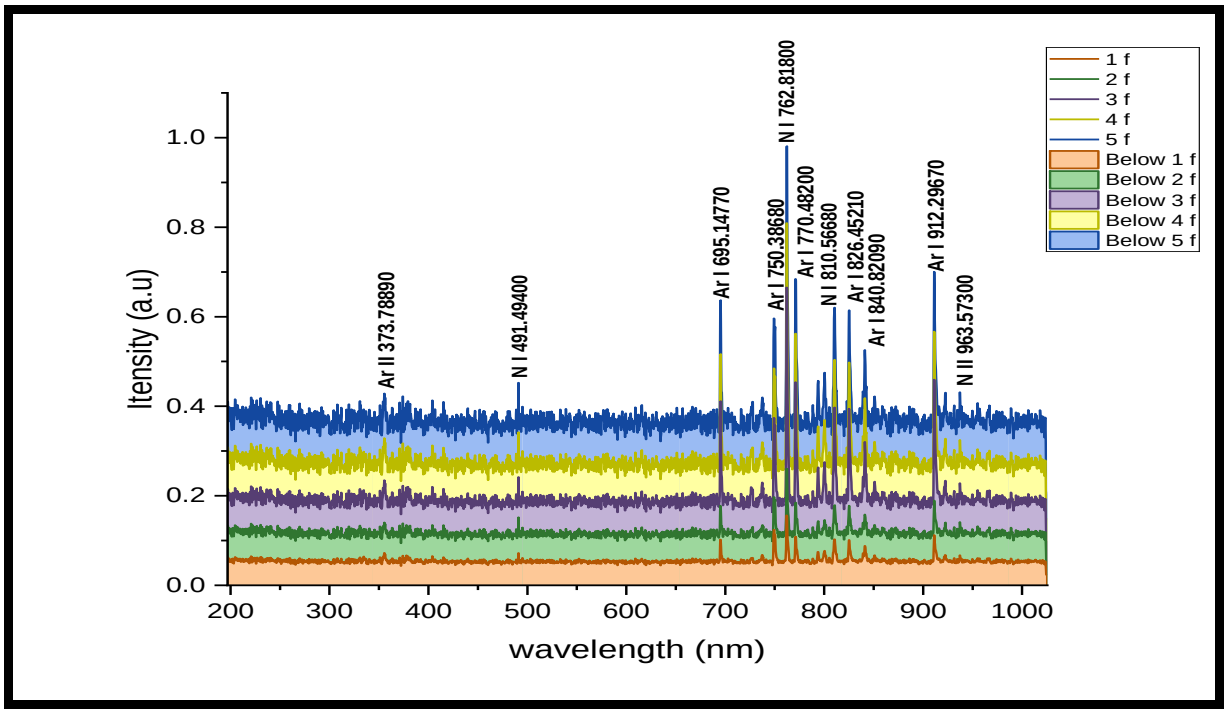

Figure 2: Relationship between Optical Emission Spectra for argon and Gas Flow Rate for a Plasma Jet, where the voltage is 10 KV, and the change in gas flow value is between 1 to 5 L/min.

In Figure 3, there are multiple peaks of nitrogen gas observed in the spectrum, with most of them matching the data from the Higher Institute (NIST) . At all values of the applied gas flow, the nitrogen gas (N2 II) exhibits its highest peak on the spectrum at a wavelength of 359.35970 nm. When the voltage is 10 KV and the flow changes between 5 and 9 L/min, the highest peak for nitrogen gas (N2 I) occurs at a wavelength of 381.82680 nm. The majority of plasma peaks were observed within the wavelength range of (300–1000) nm.

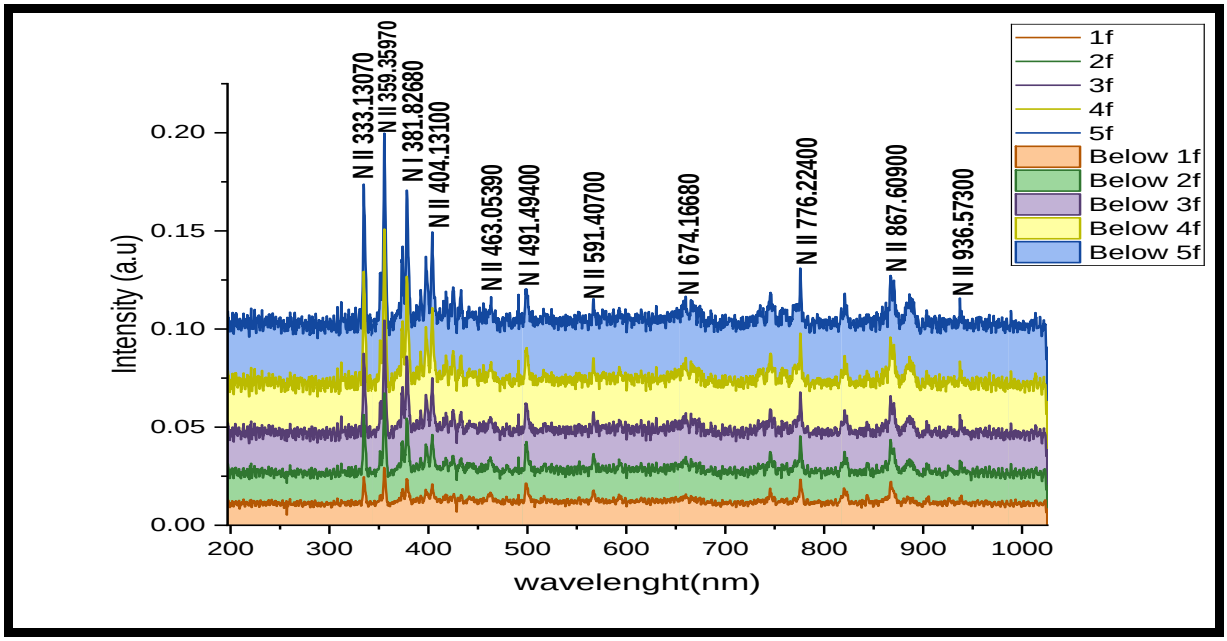

Figure 3: Relationship between Optical Emission Spectra for nitrogen and Gas Flow Rate for a Plasma Jet, where the voltage is 10 KV, and the change in gas flow value is between 5 to 9L/min.

As illustrated in Figure 4, air is a mixture of gases consisting primarily of 78% nitrogen and roughly 21% oxygen. Therefore, it is natural for peaks for both elements to appear in the spectrum, with the highest peak for nitrogen (N II) at a wavelength of 776.22400 nm and the highest peak for oxygen (O II) at a wavelength of 355.8590 nm.

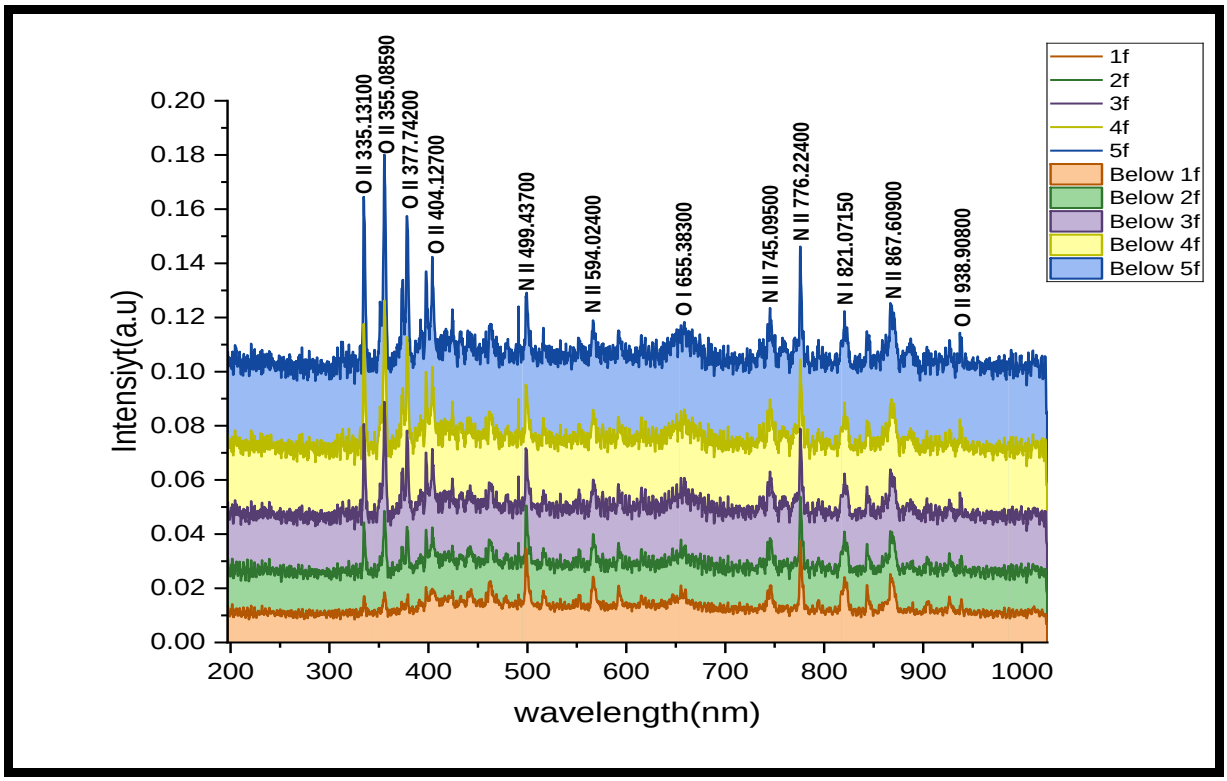

Figure 4: Relationship between Optical Emission Spectra for air and Gas Flow Rate for a Plasma Jet, where the voltage is 10 KV, and the change in gas flow value is between 4 to 8 L/min.

We notice from Figures 2, 3, and 4 that we need higher amounts of gas flow when analyzing the spectrum of air and nitrogen compared to the amount of gas used to analyze the spectrum of argon. The reason for this is that air and nitrogen contain high percentages of oxygen and nitrogen, which are gases with a similar molecular structure. This molecular structure indicates the presence of more intricate energy levels resulting from chemical reactions and various emissions. In the analysis of air and nitrogen spectra, increased overlap across spectral lines may enhance the chemical interactions between the various components. Consequently, it is vital to augment the gas flow to get better and more precise spectrum indications. Conversely, the analysis of the argon spectrum experiences less interference owing to argon's monatomic nature, which mitigates chemical effects and intricate interactions. Consequently, the spectra of argon gas may be obtained with reduced gas flow compared to the analysis of air and nitrogen spectra.

Figures 5,6 and 7 demonstrate the $ln[\frac{\lambda ji\ I_{ji}}{hc\ A_{ji} g_j}]$ as a function of (E_j). The electron temperature (T_e) Which is associated with the slope of the fitting (slope=m=$\frac{-1}{KT}$) Also, the broadening of Gausin was neglected because it is very small, Whereas Stark broadening was used to compute the electron density (ne)

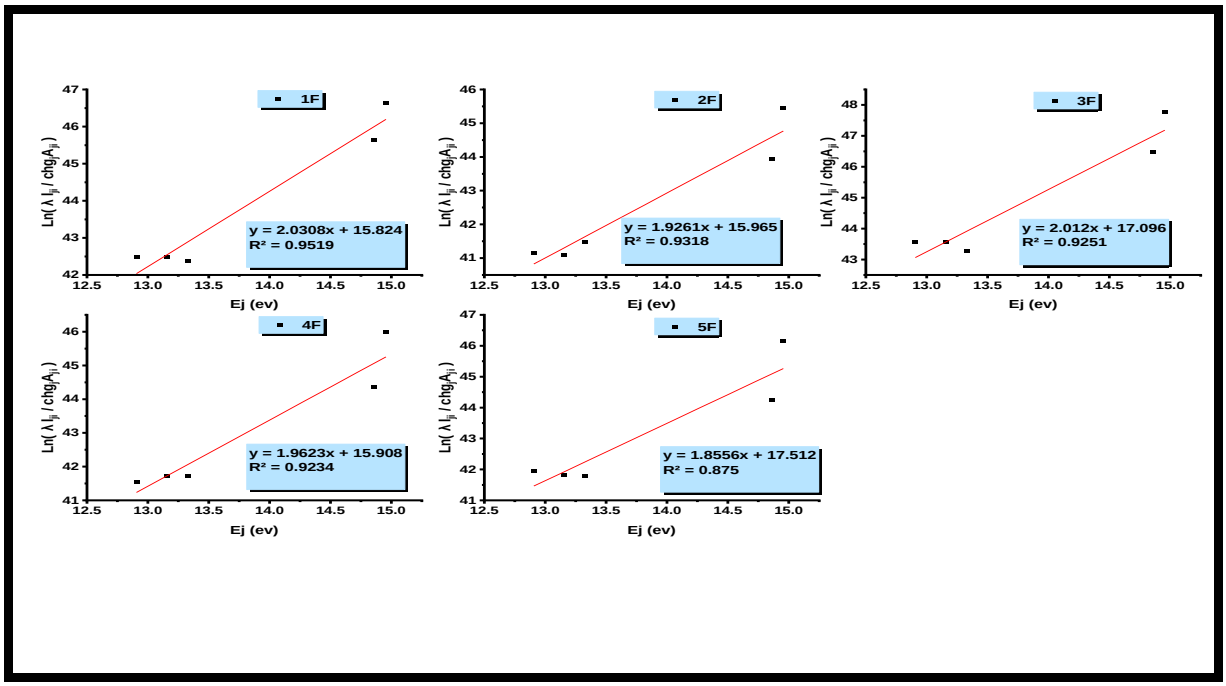

Figure (5): Boltzmann diagrams for argon at various gas flow rates (ranging from 1 to 5 L/min).

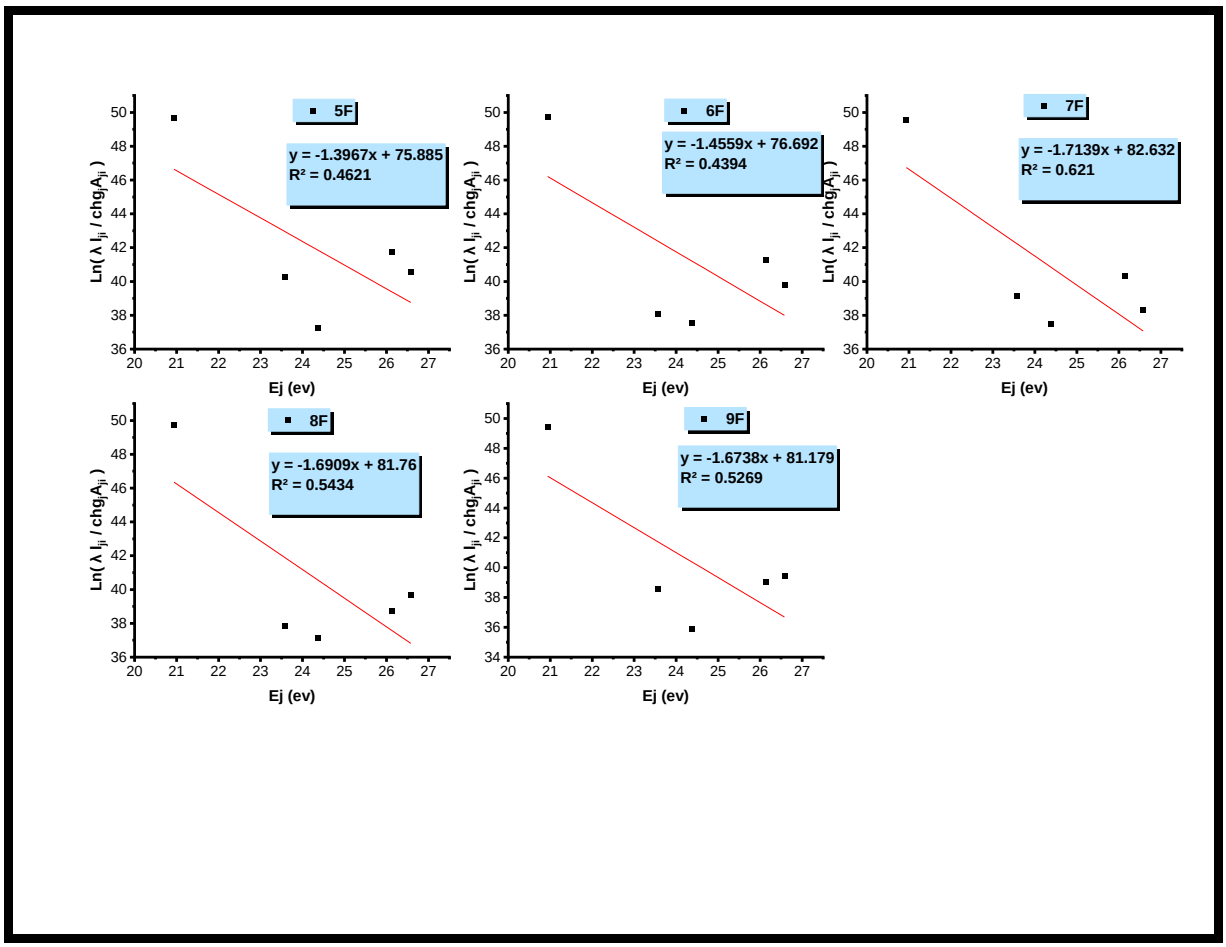

Figure (6): Boltzmann diagrams for nitrogen at various gas flow rates (ranging from 5 to 9 L/min).

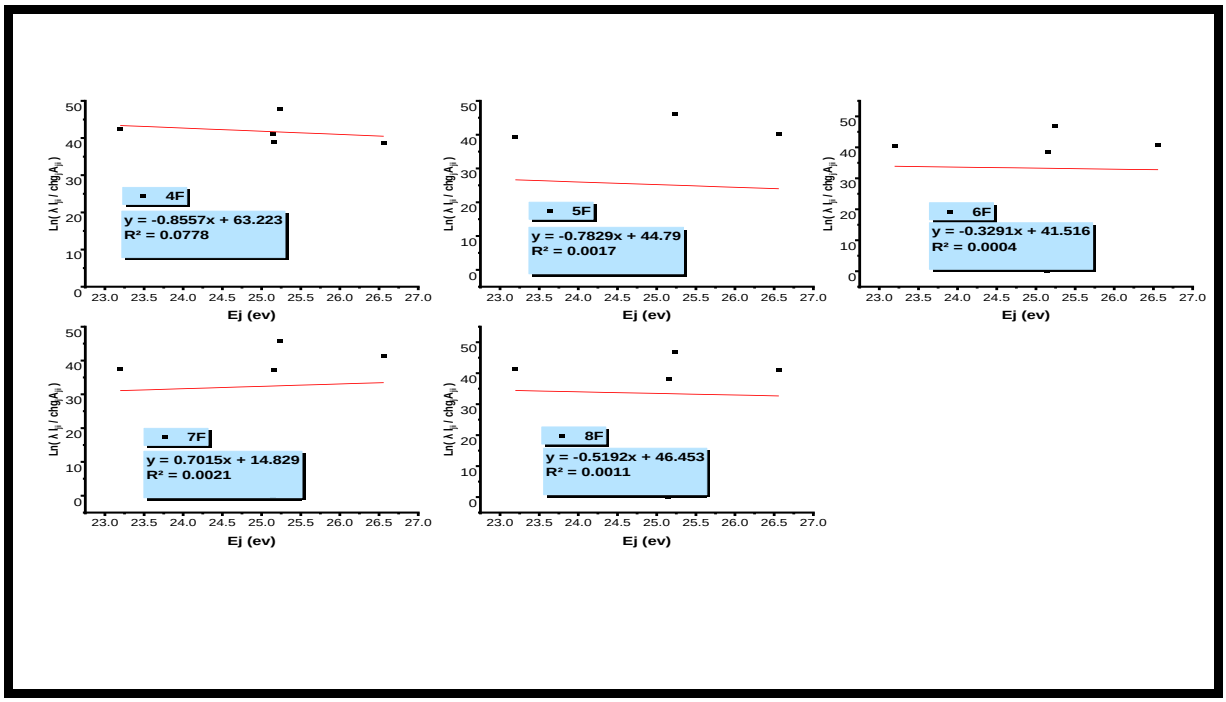

Figure (7): Boltzmann diagrams for air at various gas flow rates (ranging from 4 to 8 L/min).

Figure 8 displays the Voigt fitting for argon, incorporating Stark and Gaussian broadening at the peak of the Ar I line at 695.14770 nm, for different gas flow rates. Figure 9 exhibits the Voigt fitting for nitrogen at the peak of the N II line at 404.13100 nm, for various gas flow rates. Figure 10 illustrates the Voigt fitting for air at the peak of the N II line at 776.22400 nm, for different gas flow rates. These figures were utilized to ascertain the electron density.

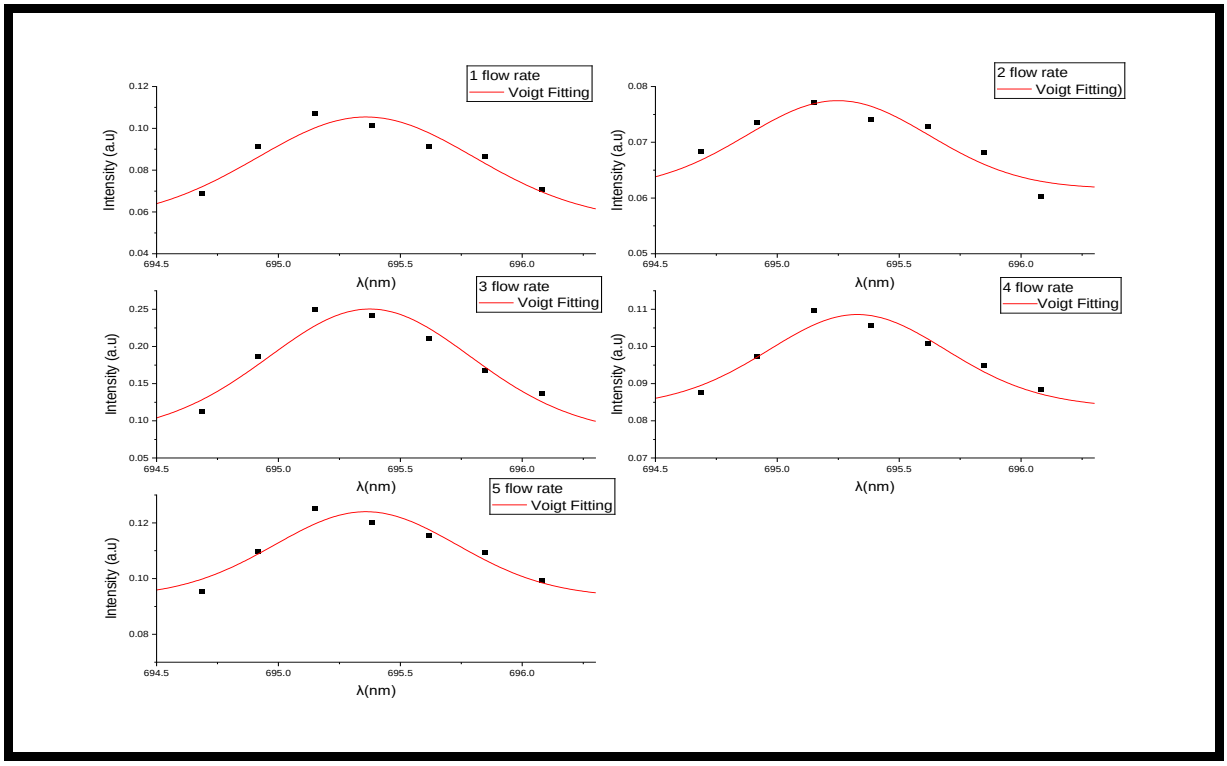

Figure (8): Voigt fitting for argon line of Ar I at 695.14770 nm.

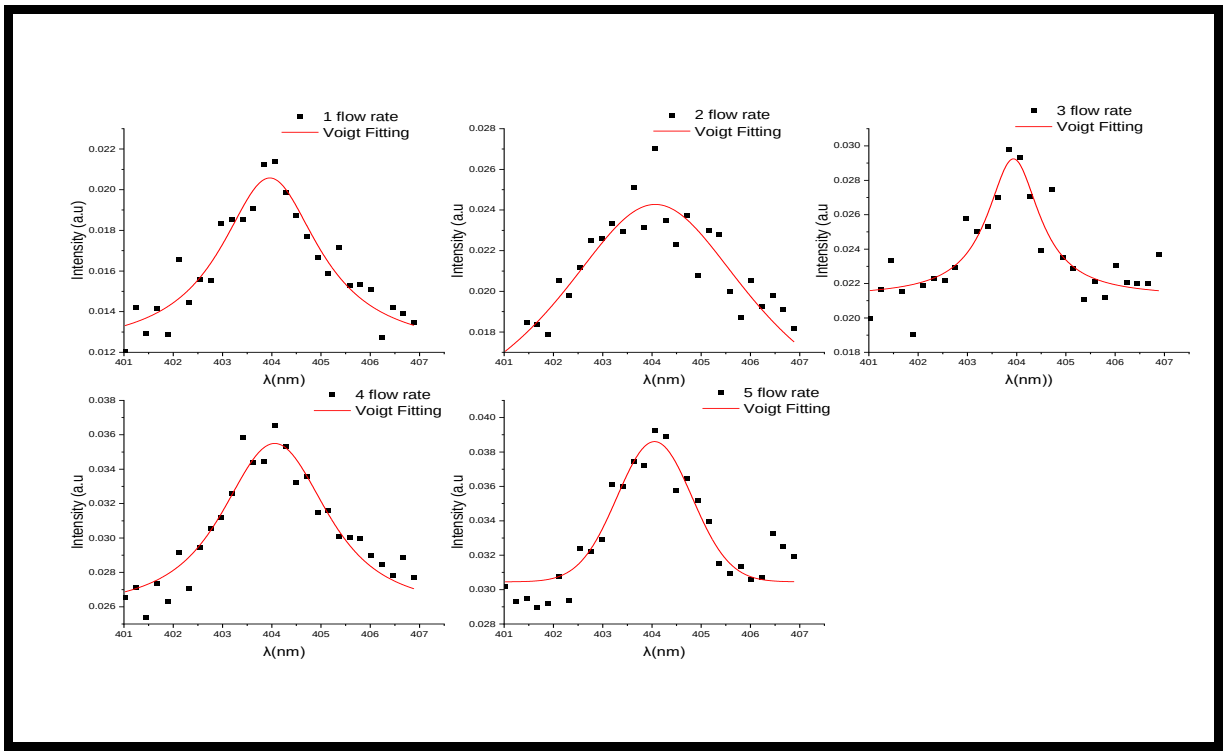

Figure (9): Voigt fitting for nitrogen line of N II at 404.13100 nm.

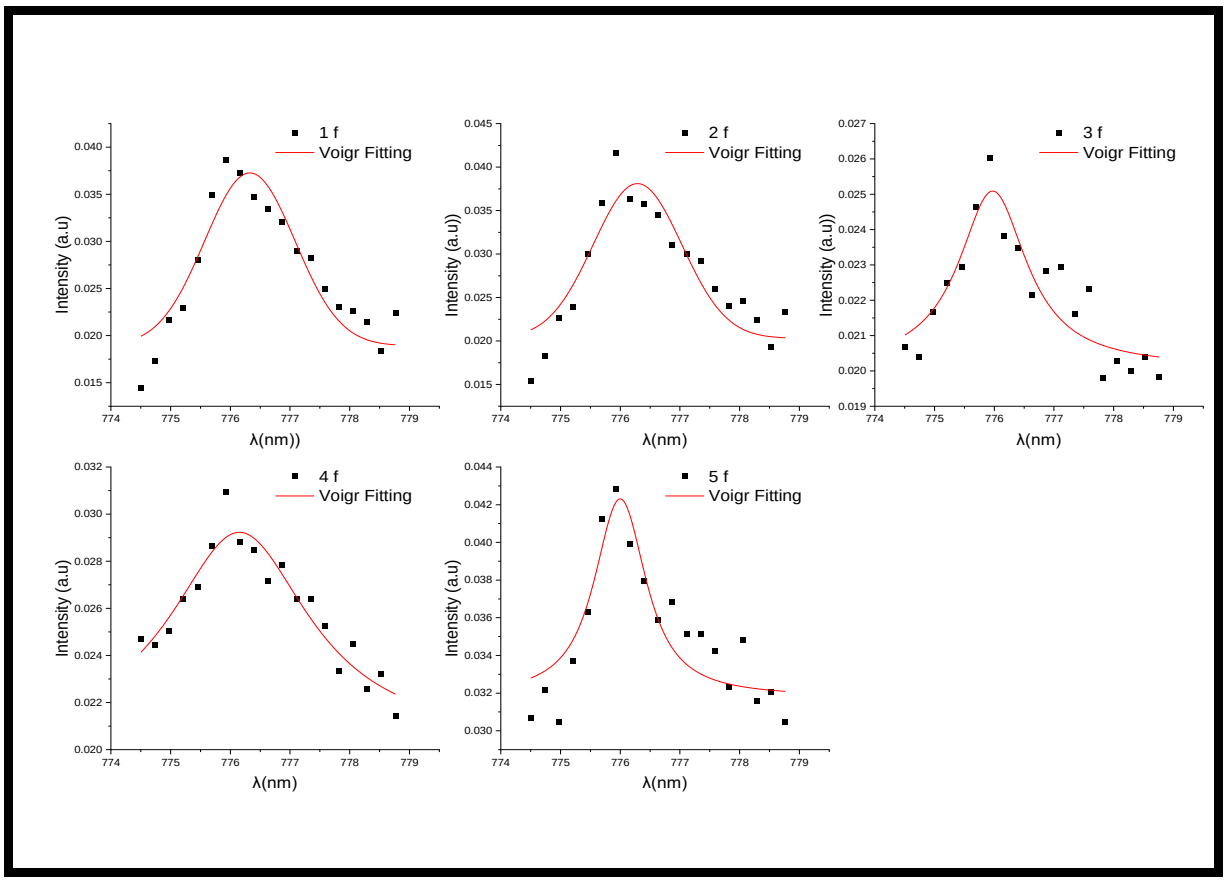

Figure (10): Voigt fitting for air line of N II at 776.22400 nm.

We can observe from Figures (11, 12, 13) and Tables 1, 2 and 3 that the electron temperature in argon is almost constant and shows a slight increase with increasing flux, while the electron density shows a slight decrease. The electron temperature and density of nitrogen change more with flow rate. In the case of air, the electron temperature fluctuates greatly with different flow rates, while the electron density appears to change less.

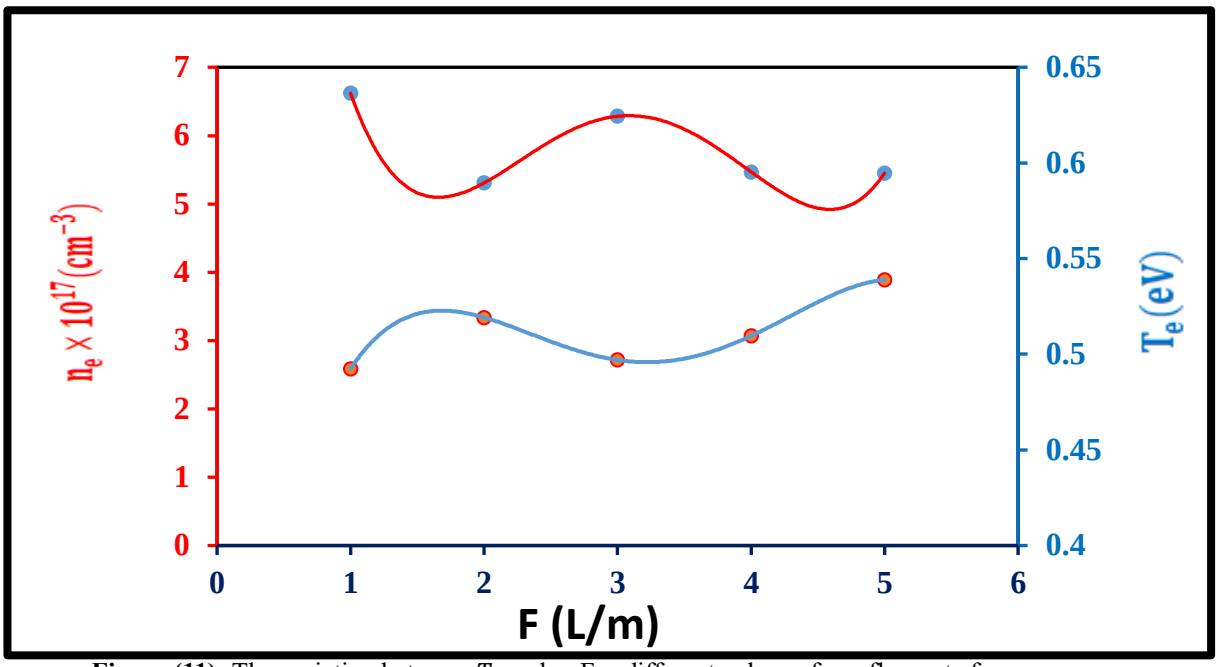

Figure (11): The variation between T_e and n_eFor different values of gas flow rate for argon.

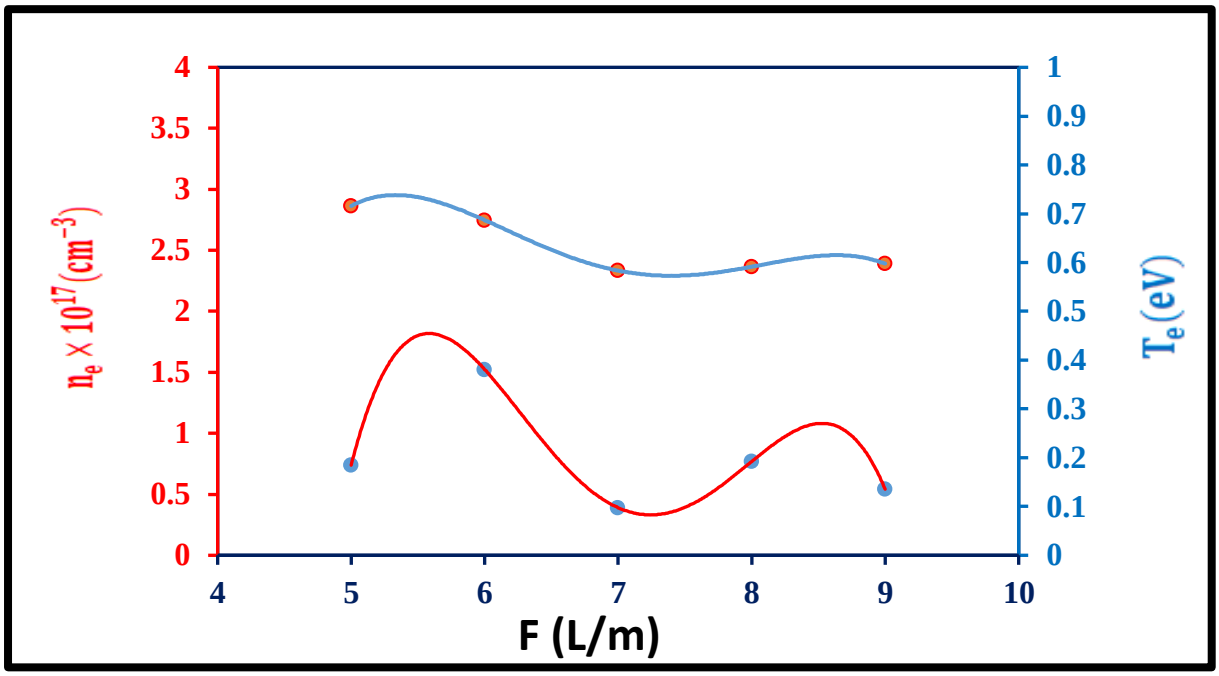

Figure (12): The variation between T_e and n_eFor different values of gas flow rate for nitrogen.

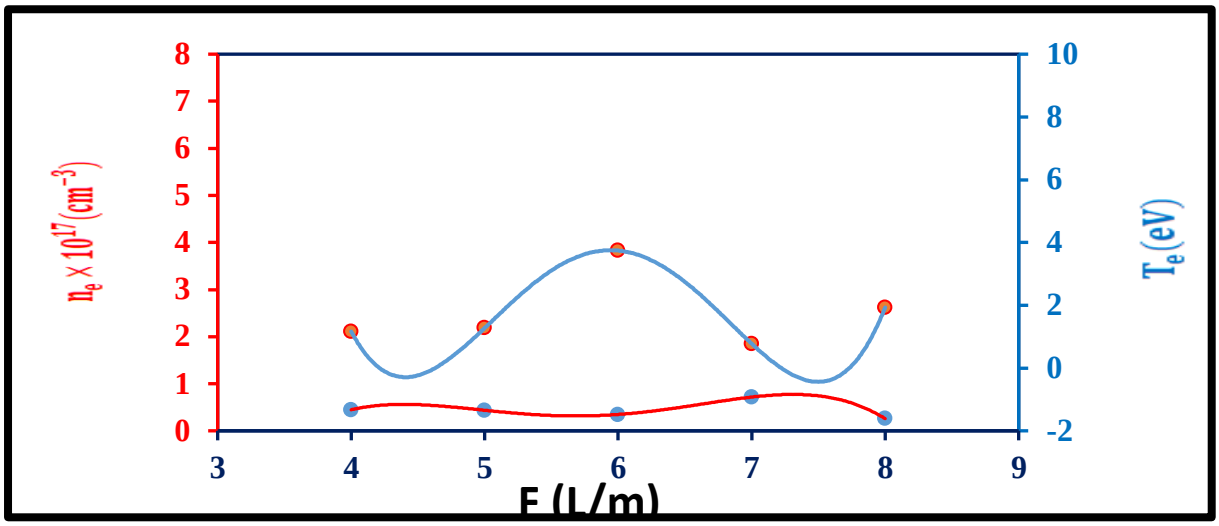

Figure (13): The variation between T_e and n_eFor different values of gas flow rate for air.

Tables 1, 2 and 3 provide a summary of how gas flow rate for different gas types affects plasma properties.

Table (1): - Argon plasma parameters for the different gas flow values.

F (L/M)	$T_e(e_v)$	$n_e * 10^{17}(cm^{-3})$	FWHM (nm)	$f_p\,(Hz)10^{12}$	$\lambda_D * 10^{-6}(cm)$
1	0.492416782	6.620361446	1.09898	23.1453	2.026349651
2	0.519183843	5.307650602	0.88107	20.7240	2.323797259
3	0.497017893	6.282228916	1.04285	22.5465	2.089863625
4	0.509606075	5.468915663	0.90784	21.0365	2.268065011
5	0.538909248	5.448614458	0.90447	20.9974	2.336703411

Table (2): - Nitrogen plasma parameters for the different gas flow values.

F (L/M)	$T_e(e_v)$	$n_e * 10^{17}(cm^{-3})$	FWHM (nm)	$f_p\,(Hz)10^{12}$	$\lambda_D * 10^{-6}(cm)$
5	0.715973366	0.737972727	2.43531	7.7276	7.318415978
6	0.686860361	1.522860606	5.02544	11.1008	4.989912895
7	0.583464613	0.390393939	1.2883	5.6205	9.083318463
8	0.591401029	0.769157576	2.53822	7.8891	6.515116572
9	0.597442944	0.541615152	1.78733	6.6201	7.803539436

Table (3): - Air plasma parameters for the different gas flow values.

F (L/M)	$T_e(e_v)$	$n_e * 10^{17}(cm^{-3})$	FWHM (nm)	$f_p\,(Hz)10^{12}$	$\lambda_D * 10^{-6}(cm)$
4	1.168633867	0.445917959	1.78278	6.0069	12.02819793
5	1.277302337	0.43644072	1.74489	5.9427	12.71080439
6	3.741114852	0.348049025	1.3915	5.3096	21.95354516
7	0.77309625	0.716953477	2.86638	7.6167	10.47682015

8	1.926040062	0.259092046	1.03585	4.5788	20.2579004

Discuss the results

Analysis of Plasma Jet Characteristics: Impact of Gas Type and Gas Flow Rates

This study provides a comprehensive analysis of the effects of physical factors on plasma jet characteristics, focusing on electron temperature (T_e) and electron density (n_e). The results, supported by detailed spectral analysis and corresponding tables, offer valuable insights into plasma behavior, which are crucial for various industrial, medical, and environmental applications.

1 .Plasma Characteristics Based on Gas Type

A. Argon Plasma:

Electron Temperature: (T_e)

Increases gradually from 0.492, eV at 1 L/min to 0.539, eV at 5 L/min.

Electron Density (n_e)

Decreases from 6.62 $\times$ $\mathbf{10^{17}}(\mathbf{cm^{-3}})$ at 1 L/min to 5.45 $\times$ $\mathbf{10^{17}}(\mathbf{cm^{-3}})$at 5 L/min.

Argon's simple atomic structure facilitates stable plasma behavior. Increasing the gas flow reduces electron-neutral interaction time, causing a decrease in n_e while maintaining a steady increase in T_e . These properties make argon suitable for thermal applications requiring stability.

B. Nitrogen Plasma:

Electron Temperature (T_e):

Decreases from 0.716, eV at 5 L/min to 0.597, eV at 9 L/min.

Electron Density (n_e):

Peaks at 1.52 $\times$ $\mathbf{10^{17}}(\mathbf{cm^{-3}})$ at 6 L/min and decreases to 0.54$\times$ $\mathbf{10^{17}}(\mathbf{cm^{-3}})$at 9 L/min.

Nitrogen's diatomic molecular structure requires substantial energy for dissociation, leading to a decline in T_e. The peak n_e at 6 L/min represents optimal conditions for ionization. At higher flow rates, reduced interaction time diminishes ionization efficiency, lowering n_e .

C. Air Plasma:

Electron Temperature (T_e):

Peaks at 3.741, eV at 6 L/min, drops to at 0.773eVat 7 L/min, and rises to 1.926, eV at 8 L/min.

Electron Density (n_e):

Peaks at 0.72 $\times$ $\mathbf{10^{17}}(\mathbf{cm^{-3}})$ at 7 L/min and drops to 0.26 $\times$ $\mathbf{10^{17}}(\mathbf{cm^{-3}})$ at 8 L/min.

Air, as a mixture of nitrogen and oxygen, exhibits complex plasma behavior. Oxygen's higher reactivity and nitrogen's molecular interactions cause significant fluctuations in T_e and n_e . These properties make air plasma versatile for applications requiring dynamic plasma interactions, such as environmental cleaning.

From the previous results, we notice the effect of both the gas type and the flow, as follows:

A Effect of Gas Type:

Argon: Stable plasma behavior due to its atomic simplicity, with gradual changes in T_e and n_e. Ideal for processes requiring thermal control, such as laser welding.

Nitrogen: Sensitive to flow rate changes, with noticeable declines in T_e and n_e at higher rates. Useful in chemical plasma applications like surface nitriding.

Air: Exhibits dynamic changes in plasma properties due to its composite nature. Suitable for applications demanding chemical versatility.

B. Effect of Flow Rate:

Lower Flow Rates: Promote better ionization efficiency, especially in nitrogen plasma, resulting in higher n_e .

Higher Flow Rates: Increase energy transfer efficiency but reduce n_e due to shortened interaction time. Fluctuations in air plasma at higher rates highlight the complex interplay between its components.

The prior results indicate that argon plasma is well suited for thermal applications necessitating stability and precise control. Nitrogen plasma is efficacious for chemical applications involving active molecular processes.Air plasma is adaptable and suitable in dynamic settings, including sterilization and environmental remediation.

This research underscores the critical role of gas type and flow rate in defining plasma properties, providing a foundation for tailored plasma applications in various domains.

4- Conclusion

This study investigates the effect of gas flow rate on the plasma parameters of an atmospheric pressure plasma jet using optical emission spectroscopy (OES). The research examines three gases: argon, nitrogen, and air, to evaluate their impact on electron temperature () and electron density (). Atmospheric pressure plasma jets are effective in generating non-thermal plasma, which has applications in surface modification, environmental cleaning, and sterilization. OES is employed to measure plasma properties, revealing that noble gases like argon exhibit stable behavior due to limited chemical reactivity, whereas reactive gases like nitrogen and air show significant variations caused by complex molecular interactions.

The results indicate that electron temperature generally increases with flow rate in argon but decreases in nitrogen, reflecting the energy demands of molecular dissociation. Air plasma displays highly dynamic behavior due to the interplay between nitrogen and oxygen components. Electron density decreases with higher flow rates in all gases, with nitrogen and air showing sharper declines due to reduced ionization efficiency. These findings provide insights into optimizing gas type and flow rate for specific plasma applications, enhancing their efficiency in industrial, medical, and environmental fields. The study highlights the versatility of non-thermal plasma systems and their potential for tailored applications.

References

[1] W. I. Yaseen, "The Electron Temperature and the Electron Density Measurement by Optical Emission Spectroscopy in Laser Produced Aluminum Plasma in Air," Iraqi Journal of Science. 57 (2C),1584-1590 (2016).
https://ijs.uobaghdad.edu.iq/index.php/eijs/article/view/7235?articlesBySimilarityPage=1

[2] O. A. Hammadi et al., "Employment of Magnetron to Enhance Langmuir Probe Characteristics of Argon Glow Discharge Plasma in Sputtering System," Iraqi Journal of Applied Physics. 12 (4),19-28 (2016).
https://www.iasj.net/iasj/download/f19200620a094a9e

[3] O. A. Hammadi, "Synthesis and Characterization of Polycrystalline Carbon Nitride Nanoparticles by Fast Glow Discharge-Induced Reaction of Methane and Ammonia," Advanced Science, Engineering and Medicine. 11 (5), 346-350 (2019).
https://www.researchgate.net/publication/331453074_Synthesis_and_Characterization_of_Polycrystalline_Carbon_Nitride_Nanoparticles_by_Fast_Glow_Discharge-Induced_Reaction_of_Methane_and_Ammonia

[4] Sura A. Kadhim, Hammad R. Humud, "Development of Low-Temperature Atmospheric Plasma Jet Sources for Biological Applications," Iraqi Journal of Science. 64,4262–4272 (2023).
https://iasj.net/iasj/article/281510

[5] Domonkos, M., Tichá, P., Trejbal, J., & Demo, P. Applications of Cold Atmospheric Pressure Plasma Technology in Medicine, Agriculture and Food Industry. Applied Sciences, vol. **11**, p. 4809, (2021).
https://doi.org/10.3390/app11114809

[6] A. Bogaests, E. Neyts R. Gijbels, and J.V. Mullen; Spectrochimic Acta PartB; 57 609 – 658 (2002).
https://doi.org/10.1016/S0584-8547(01)00406-2.

[7] Sharma, S., Chalise, R., Basnet, S., Lamichhane, H.P., & Khanal, R. Development of a low-cost plasma source using fly-back transformer for atmospheric pressure gliding arc discharge. Physics of Plasmas, vol. **28**, p. 053502, (2021).
https://doi.org/10.1063/5.0187159

[8] Wang, T., Wang, J., Wang, S., Lv, L., Li, M., & Shi, L. Effect of metal mesh addition on polymer surface etching by an atmospheric pressure plasma jet. Applied Surface Science, 570, 151258 (2021).

https://doi.org/10.1016/j.apsusc.2021.151258

[9] K. Kitano, H. Furusha, Y. Nagasaki, S. Ikawa, and S. Hamaguchi, 28th International Conference on Phenomena in Ionized Gases It was held in Prague, the capital of the Czech Republic Republic, 1131 – 1134, (2007).
http://doi:10.1088/0963-0252/17/2/020201

[10] A. Shashurin, M. Keidar, S. Bronnikov, R. A. Jurjus, and M. A. Stepp, Applied Physics Letters; 93, 181501, (2008), 1-3.
https://doi.org/10.1063/1.3020223

[11] Lackmann, J. W., Bruno, G., Jablonowski, H., Kogelheide, F., Offerhaus, B., Held, J., ... & Wende, K. Nitrosylation vs. oxidation–How to modulate cold physical plasmas for biological applications. PLoS One, **14**(5), e0216606 (2019).
https://doi.org/10.1371/journal.pone.0216606

[12] Patrakova, E., Biryukov, M., Troitskaya, O., Gugin, P., Milakhina, E., Semenov, D., ... & Koval, O. Chloroquine Enhances Death in Lung Adenocarcinoma A549 Cells Exposed to Cold Atmospheric Plasma Jet. Cells, **12**(2), 290 (2023).
https://doi.org/10.3390/cells12020290

[13] Bekeschus, S., Poschkamp, B., & van der Linde, J. Medical gas plasma promotes blood coagulation via platelet activation. Biomaterials, **278**, 120433 (2021).
https://doi.org/10.1016/j.biomaterials.2020.120433

[14] Yoshimura, S., Otsubo, Y., Yamashita, A., & Ishikawa, K. Insights into normothermic treatment with direct irradiation of atmospheric pressure plasma for biological applications. Japanese Journal of Applied Physics, **60**(1), 010502 (2020).
https://doi.org/10.35848/1347-4065/abcbd2

[15] Emelyanov, Oleg A., Efrem G. Feklistov, Natalia V. Smirnova, Konstantin A. Kolbe, Evgeniy V. Zinoviev, Marat S. Asadulaev, Andrey A. Popov, Anton S. Shabunin, and Kamal F. Osmanov. Corona discharge plasma application for in vitro modulation of fibroblast proliferation and wound healing. In AIP Conference Proceedings, vol. **2179**, no. 1. AIP Publishing, (2019).
https://doi.org/10.1063/1.5135479

[16] Lou, B.S., Hsieh, J.H., Chen, C.M., Hou, C.W., Wu, H.Y., Chou, P.Y., Lai, C.H. and Lee, J.W. Helium/argon-generated cold atmospheric plasma facilitates cutaneous wound healing. Frontiers in bioengineering and biotechnology, **8**, p.683 (2020).
https://doi.org/10.3389/fbioe.2020.00683

[17] Darmawati, S., Rohmani, A., Nurani, L.H., Prastiyanto, M.E., Dewi, S.S., Salsabila, N., Wahyuningtyas, E.S., Murdiya, F., Sikumbang, I.M., Rohmah, R.N. and Fatimah, Y.A. When plasma jet is effective for chronic wound bacteria inactivation, is it also effective for wound healing? Clinical Plasma Medicine, **14**, p.100085 (2019).
https://doi.org/10.1016/j.cpme.2019.100085

[18] Rad, Z.S. and Davani, F.A. Measurements of the electrical parameters and wound area for investigation on the effect of different non-thermal atmospheric pressure plasma sources on wound healing time. Measurement, **155**, p.107545 (2020).
https://doi.org/10.1016/j.measurement.2020.107545

[19] Darmawati, Sri, Nasruddin Nasruddin, Putri Kurniasiwi, A. H. Mukaromah, Arya Iswara, Gela Setya Ayu Putri, H. S. E. Rahayu et al. Plasma jet effectiveness alteration in acute wound healing by binahong (Anredera cordifolia) extract. Plasma Medicine **10**, no. 4 (2020).
https://doi.org/10.1615/plasmamed.2021037264

[20] Lotfy, Khaled. The impact of the carrier gas composition of non-thermal atmospheric pressure plasma jet for bacteria sterilization. AIP Advances **10**, no. 1 (2020).
https://doi.org/10.1063/1.5099923

[21] Thana, P., Kuensaen, C., Poramapijitwat, P., Sarapirom, S., Yu, L. and Boonyawan, D. A compact pulse-modulation air plasma jet for the inactivation of chronic wound bacteria: Bactericidal effects & host safety. Surface and Coatings Technology, **400**, p.126229 (2020).
https://doi.org/10.1016/j.surfcoat.2020.126229

[22] Liu, G., Shi, F., Wang, Q., Zhang, Z., Guo, J. and Zhuang, J. Penetration effect of the kINPen plasma jet investigated with a 3D agar-entrapped bacteria model. Microchemical Journal, **183**, p.107973 (2022).
https://doi.org/10.1016/j.microc.2022.107973

[23] Lata, S., Chakravorty, S., Mitra, T., Pradhan, P.K., Mohanty, S., Patel, P., Jha, E., Panda, P.K., Verma, S.K. and Suar, M. Aurora Borealis in dentistry: The applications of cold

plasma in biomedicine. Materials Today Bio, **13**, p.100200 (2022).
https://doi.org/10.1016/j.mtbio.2021.100200

[24] Hammad R. Humud, Qusay A. Abbas and Khansaa Fadhil Abdullah. “Tooth bleaching by plasma jet assisted by hydrogen peroxide and water." Der Pharmacia Lettr.; **8**, 12 (2016) 229-233 (2016).
http://scholarsresearchlibrary.com/archive.html

[25] Whiley, H., Keerthirathne, T.P., Kuhn, E.J., Nisar, M.A., Sibley, A., Speck, P. and Ross, K.E. Efficacy of the PlasmaShield®, a non-thermal, plasma-based air purification device, in removing airborne microorganisms. Electrochem, **3**(2), pp.276-284 (2022).
https://doi.org/10.3390/electrochem3020019

[26] Zouzelka, R., Olejnicek, J., Ksirova, P., Hubicka, Z., Duchon, J., Martiniakova, I., Muzikova, B., Mergl, M., Kalbac, M., Brabec, L. and Kocirik, M. Hierarchical TiO2 Layers Prepared by Plasma Jets. Nanomaterials, **11**(12), p.3254 (2021).
https://doi.org/10.3390/nano11123254

[27] Hammad R. Humud, Maha Adel Mahmood , Wafaa Abd Al-Razaq.“Strain specificity in antimicrobial activity of non-thermal plasma", Iraqi Journal of Physics; **11**, 20 110-115 (2013)
http://ijp.uobaghdad.edu.iq/index.php/physics/article/view/388

[28] Hammad R. Humud , Ahamad S. Wasfi , Wafaa Abd Al-Razaq, Mazin S. El-Ansary. “Argon plasma needle source".Iraqi Journal of Physics ;**10**, 17 53-57 (2012).
https://ijp.uobaghdad.edu.iq/index.php/physics/article/view/772

[29] Hiba M. Abdulwahab,Hammad R. Humud.“Diagnostic a Microwave Plasma Jet System for Laboratory Applications."AIP conference proceedings, December (2023).
https://doi.org/10.1063/5.0183707

[30] S. Iordanova, I. Koleva, "Optical emission spectroscopy diagnostics of inductively-driven plasmas in argon gas at low pressures," Spectrochimica Acta Part B. 62, 344–356 (2007).
https://doi.org/10.1016/j.sab.2007.03.026

[31] M. Ahmed Baida, "Plasma Parameters Generated from Iron Spectral Lines by Using LIBS Technique," IOP Conf. Series: Materials Science and Engineering. 928, 1-11 (2020).
https://iopscience.iop.org/article/10.1088/1757-899X/928/7/072096/pdf

[32] Fatima K. Hammoud, Kadhim A. Aadim, "Measurements and Calculations of Parameters of Zinc Oxide Plasma Produced by Laser-Induced Breakdown Spectroscopy," Iraqi Journal of Science. 63, 1540–1548 (2022).
https://doi.org/10.24996/ijs.2022.63.4.14

[33] Hadeel K. Nasif, Kadhim A. Aadim, Baida M. Ahmed, "Comparison Study Between Spectroscopic Analysis For (ZN SN.) Plasma By Libs," MINAR International Journal of Applied Sciences and Technology. 3, 52-61 (2021).
http://dx.doi.org/10.47832/2717-8234.2-3.7

[34] Haider Abdulrida, Qusay Adnan Abbas, "Effect of Using Nanoscale Titanium as a Target Instead of a Bulk Target on Laser-Induced Plasma Properties," Journal of Survey in Fisheries Sciences. 10, 128-140 (2023).
https://doi.org/10.17762/sfs.v10i3S.19

[35] L. Oks, "Effect of thermal collective modes on the Stark broadening of spectral lines in strongly coupled plasmas," J. Phys. B At. Mol. Opt. Phys. 49 (6), (2016).
http://dx.doi.org/10.1088/0953-4075/49/6/065701

[36] Zahraa Mohammed Hasan, Qusay Adnan Abbas, "Influence of AC Frequency on Hollow Magnetron Sputtering Discharge Parameters," Iraqi Journal of Physics. 22, 31-41 (2024).
https://doi.org/10.30723/ijp.v22i1.1191

[37] R. Yagi, R. Pandey, K. Kumar, R.S. Srivastava, "Effect of electric and magnetic field on welding parameters in plasma welding," Int. J. Eng. Sci. Technol. 3 (8), 168–176 (2011).
https://www.ajol.info/index.php/ijest/article/view/80182/70441

[38] Maryam M. Shehab, Kadhim A. Aadim, "Spectroscopic Diagnosis of the CdO: CoO Plasma Produced by Nd: YAG Laser," Iraqi Journal of Science. 62, 2948–2955 (2021).
https://doi.org/10.24996/ijs.2021.62.9.11

[39] F. Faubert, M. Wartel, N. Pellerin, S. Pellerin, V. Cochet, E. Regnier, B. Hnatiuc, "Treatment by gliding arc of epoxy resin: Preliminary analysis of surface modifications," In Advanced Topics in Optoelectronics Microelectronics and Nanotechnologies VIII; International Society for Optics and Photonics: Bellingham, WA, USA. 10010, 100103G (2016).

http://dx.doi.org/10.1117/12.2257535
[40] Hiba Qassim, Saba J. Kadhem, "Study the Effect of Dielectric Barrier Discharge (DBD) Plasma on the Decomposition of Volatile Organic Compounds," Iraqi Journal of Physics. 20, 45-53 (2022).https://ijp.uobaghdad.edu.iq/index.php/physics/article/view/1056